Journal of Sound and Vibration (1999) **224**(2), 359–374
Article No. jsvi.1999.2163, available online at http://www.idealibrary.com on IDEAL®

APPLICATION OF THE STRAIN ENERGY DAMAGE DETECTION METHOD TO PLATE-LIKE STRUCTURES

P. CORNWELL

Rose Hulman Institute of Technology, 5500 *Wabash Ave*., *Terre Haute*, *IN* 47805, *U.S.A.*

AND

S. W. DOEBLING AND C. R. FARRAR

Los Alamos National Laboratory, *ESA-EA*, *MS P*946, *Los Alamos*, *NM* 87545, *U.S.A.*

(*Received* 10 *August* 1998, *and in final form* 8 *February* 1999)

In this paper the problem of using measured modal parameters to detect and locate damage in plate-like structures is investigated. Many methods exist for locating damage in a structure given the modal properties before and after damage. Unfortunately, many of these methods require a correlated finite element model or mass normalized mode shapes. If the modal properties are obtained using ambient excitation then the mode shapes will not be mass normalized. In this paper a method based on the changes in the strain energy of the structure will be discussed. This method was originally developed for beam-like structures, that is, structures characterized by one-dimensional curvature. In this paper the method will be generalized to plate-like structures that are characterized by two-dimensional curvature. This method only requires the mode shapes of the structure before and after damage. To evaluate the effectiveness of the method it will be applied to both simulated and experimental data.

1. INTRODUCTION

Significant work has been done in the area of detecting damage in structures using changes in the dynamic response of the structure. Because the natural frequencies and mode shapes of a structure are dependent on the mass and stiffness distributions, any subsequent changes in them should, theoretically, be reflected in changes in the frequency and mode shapes of the structure. The problem of using measured frequencies and mode shapes and their sensitivity to damage is a question not to be addressed in this paper. An extensive literature review [1] of the state of the art of damage detection and health monitoring from vibration characteristics has recently been published. From this review it is clear that there are a large number of proposed methods of detecting damage from

0022–460X/99/270359 + 16 $30.00/0

vibration characteristics but, unfortunately, many of these methods require a correlated finite element model and/or mass normalized mode shapes. If the modal properties are obtained using ambient excitation, as would most likely be the case for a remote, automated health monitoring system, then the mode shapes will not be mass normalized. The method proposed in this paper avoids both of these requirements.

Pandey *et al.* [2] demonstrated that absolute changes in mode shape curvature can be a good indicator of damage for the FEM beam structure they considered. Stubbs *et al.* [3] presented a method based on the decrease in modal strain energy between two structural degrees of freedom as defined by the curvature of the measured mode shapes. This method has been successfully applied to data from a damaged bridge [4] and has been compared to several other methods [5, 6]. Several other researchers have also used changes in mode shape curvature to detect damage [7–10].

In this paper an extension of the method proposed by Stubbs *et al.* [3, 4] will be presented. This method requires that the mode shapes before and after damage be known, but the modes do not need to be mass normalized and only a few modes are required. The original formulation by Stubbs *et al.* is inherently limited to structures that are characterized by one-dimensional curvature (i.e., curvature that is uniquely a function of one independent spatial variable). In other words, the 1-D strain energy method can only be applied to structures that behave globally in a beam-like manner or can be decomposed into beam elements. (It should be noted that the 1-D strain energy method has been successfully applied to 2-D and 3-D structures, but only by decomposing them into beam-like elements.) In this paper the method will be generalized to plate-like structures that are characterized by two-dimensional curvature. To examine limitations of the method, it will be applied to several sets of simulated data and comparisons will be made between applying the original formulation to a series of slices of the structure versus the true two-dimensional formulation.

2. THEORY

For completeness the derivation of the damage indicator will be shown for both beam-like and plate-like structures.

2.1. BEAM-LIKE STRUCTURES

The strain energy of a Bernoulli–Euler beam is given by

$$U = \tfrac{1}{2}\int_0^\ell EI\left(\frac{\partial^2 w}{\partial x^2}\right)^2 \,\mathrm{d}x, \tag{1}$$

where EI is the flexural rigidity of the beam. For a particular mode shape, $\psi_i(x)$, the energy associated with that mode shape is

$$U_i = \tfrac{1}{2}\int_0^\ell EI\left(\frac{\partial^2 \psi_i}{\partial x^2}\right)^2 \,\mathrm{d}x. \tag{2}$$

If the beam is subdivided into N_d divisions as shown in Figure 1, then the

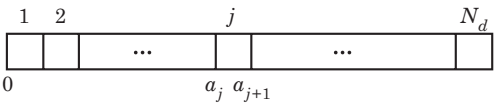

Figure 1. A schematic illustrating a beam's N_d sub-divisions.

energy associated with each sub-region j due to the ith mode is given by

$$U_{ij} = \tfrac{1}{2}\int_{a_j}^{a_{j+1}} (EI)_j \left(\frac{\partial^2 \psi_i}{\partial x^2}\right)^2 \, \mathrm{d}x. \tag{3}$$

The fractional energy is therefore

$$F_{ij} = \frac{U_{ij}}{U_i} \quad \text{and} \quad \sum_{j=1}^{N_d} F_{ij} = 1. \tag{4, 5}$$

Similar quantities can be defined for a damaged structure and are given as:

$$U_i^* = \tfrac{1}{2}\int_0^{\ell} EI^* \left(\frac{\partial^2 \psi_i^*}{\partial x^2}\right)^2 \, \mathrm{d}x, \quad U_{ij}^* = \tfrac{1}{2}\int_{a_j}^{a_{j+1}} (EI)_j^* \left(\frac{\partial^2 \psi_i^*}{\partial x^2}\right)^2 \, \mathrm{d}x, \tag{6, 7}$$

$$F_{ij}^* = \frac{U_{ij}^*}{U_i^*}, \quad \sum_{j=1}^{N_d} F_{ij} = \sum_{j=1}^{N_d} F_{ij}^* = 1, \tag{8, 9}$$

where $(\,)^*$ indicates a quantity calculated using the damaged mode shapes, ψ_i^*. By choosing the sub-regions to be relatively small, the flexural rigidity for the jth sub-region, EI_j is roughly constant and F_{ij}^* becomes

$$F_{ij}^* = (EI)_j^* \int_{a_j}^{a_{j+1}} \left(\frac{\partial^2 \psi_i^*}{\partial x^2}\right)^2 \, \mathrm{d}x / U_i^*. \tag{10}$$

If one assumes that the damage is primarily located at a single sub-region then the fractional energy will remain relatively constant in undamaged sub-regions and $F_{ij}^* = F_{ij}$. For a single damaged location at sub-region $j = k$ one finds

$$(EI)_k \int_{a_k}^{a_{k+1}} \left(\frac{\partial^2 \psi_i}{\partial x^2}\right)^2 \, \mathrm{d}x / U_i = (EI)_k^* \int_{a_k}^{a_{k+1}} \left(\frac{\partial^2 \psi_i^*}{\partial x^2}\right)^2 \, \mathrm{d}x / U_i^*. \tag{11}$$

By assuming that EI is essentially constant over the length of the beam for both the undamaged and damaged modes, equation (11) can be rearranged to give an indication of the change in the flexural rigidity of the sub-region:

$$\frac{(EI)_k}{(EI)_k^*} = \left\{ \int_{a_k}^{a_{k+1}} \left(\frac{\partial^2 \psi_i^*}{\partial x^2}\right)^2 \, \mathrm{d}x \Big/ \int_0^{\ell} \left(\frac{\partial^2 \psi_i^*}{\partial x^2}\right)^2 \, \mathrm{d}x \right\} \Big/ \left\{ \int_{a_k}^{a_{k+1}} \left(\frac{\partial^2 \psi_i}{\partial x^2}\right)^2 \, \mathrm{d}x \right.$$

$$\left. \Big/ \int_0^{\ell} \left(\frac{\partial^2 \psi_i}{\partial x^2}\right)^2 \, \mathrm{d}x \right\} \equiv \frac{f_{ik}^*}{f_{ik}}. \tag{12}$$

In order to use all the measured modes, m, in the calculation, the damage index for sub-region k is defined to be

$$\beta_k = \sum_{i=1}^{m} f_{ik}^* \Big/ \sum_{i=1}^{m} f_{ik}. \tag{13}$$

One advantage to the formulation shown in equations (12) and (13) is that the modes do not need to be normalized. Assuming that the collection of the damage indices, β_k, represent a sample population of a normally distributed random variable, a normalized damage index is obtained using

$$Z_k = (\beta_k - \bar{\beta}_k)/\sigma_k, \tag{14}$$

where $\bar{\beta}_k$ and σ_k represent the mean and standard deviation of the damage indices, respectively. In this paper it will be assumed that normalized damage indices with values greater than two are associated with potential damage locations. The preceding derivation was originally presented by Stubbs *et al.* [3, 4].

2.2. PLATE-LIKE STRUCTURES

The strain energy of a plate is given by reference [11] as:

$$U = \frac{D}{2}\int_0^b \int_0^a \left(\frac{\partial^2 w}{\partial x^2}\right)^2 + \left(\frac{\partial^2 w}{\partial y^2}\right)^2 + 2\nu\left(\frac{\partial^2 w}{\partial x^2}\right)\left(\frac{\partial^2 w}{\partial y^2}\right) + 2(1-\nu)\left(\frac{\partial^2 w}{\partial x \partial y}\right)^2 \, \mathrm{d}x \, \mathrm{d}y, \tag{15}$$

where $D = Eh^3/12(1-\nu^2)$ is the bending stiffness of the plate. For a particular mode shape, $\psi_i(x, y)$, the energy associated with that mode shape is

$$U_i = \frac{D}{2}\int_0^b \int_0^a \left(\frac{\partial^2 \psi_i}{\partial x^2}\right)^2 + \left(\frac{\partial^2 \psi_i}{\partial y^2}\right)^2 + 2\nu\left(\frac{\partial^2 \psi_i}{\partial x^2}\right)\left(\frac{\partial^2 \psi_i}{\partial y^2}\right) + 2(1-\nu)\left(\frac{\partial^2 \psi_i}{\partial x \partial y}\right)^2 \, \mathrm{d}x \, \mathrm{d}y. \tag{16}$$

If the plate is subdivided into N_x subdivisions in the x direction and N_y subdivisions in the y direction as shown in Figure 2 then the energy associated with sub-region jk for the ith mode is given by

$$U_{ijk} = \frac{D_{jk}}{2}\int_{b_k}^{b_{k+1}} \int_{a_j}^{a_{j+1}} \left(\frac{\partial^2 \psi_i}{\partial x^2}\right)^2 + \left(\frac{\partial^2 \psi_i}{\partial y^2}\right)^2 + 2\nu\left(\frac{\partial^2 \psi_i}{\partial x^2}\right)\left(\frac{\partial^2 \psi_i}{\partial y^2}\right) + 2(1-\nu)\left(\frac{\partial^2 \psi_i}{\partial x \partial y}\right)^2 \, \mathrm{d}x \, \mathrm{d}y, \tag{17}$$

so

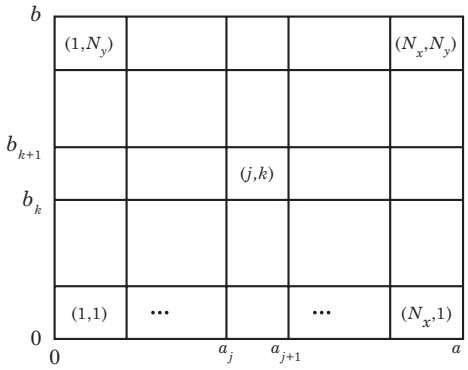

Figure 2. A schematic illustrating a plate's $N_x \times N_y$ sub-regions.

$$U_i = \sum_{k=1}^{N_s} \sum_{j=1}^{N_x} U_{ijk}, \tag{18}$$

and the fractional energy at location jk is defined to be

$$F_{ijk} = U_{ijk}/U_i \quad \text{and} \quad \sum_{k=1}^{N_y} \sum_{j=1}^{N_x} F_{ijk} = 1. \tag{19, 20}$$

Similar expressions can be written using the modes of the damaged structure, ψ_i^*. Using arguments similar to the ones used for beam-like structures a ratio of parameters can be determined that is indicative of the change of stiffness in the structure as shown in equations (21, 22):

$$D_{jk}/D_{jk}^* = f_{ijk}^*/f_{ijk}, \tag{21}$$

where

$$f_{ijk} = \frac{\int_{b_k}^{b_{k+1}} \int_{a_j}^{a_{j+1}} \left(\frac{\partial^2 \psi_i}{\partial x^2}\right)^2 + \left(\frac{\partial^2 \psi_i}{\partial y^2}\right)^2 + 2\nu \left(\frac{\partial^2 \psi_i}{\partial x^2}\right)\left(\frac{\partial^2 \psi_i}{\partial y^2}\right) + 2(1-\nu)\left(\frac{2^2 \psi_i}{\partial x dY}\right) \, \mathrm{d}x \, \mathrm{d}y}{\int_0^b \int_0^a \left(\frac{\partial^2 \psi_i}{\partial x^2}\right)^2 + \left(\frac{\partial^2 \psi_i}{\partial y^2}\right)^2 + 2\nu \left(\frac{\partial^2 \psi_i}{\partial x^2}\right)\left(\frac{\partial^2 \psi_i}{\partial y^2}\right) + 2(1-\nu)\left(\frac{\partial^2 \psi_i}{\partial x \partial y}\right)^2 \, \mathrm{d}x \, \mathrm{d}y}, \tag{22}$$

and an analogous term f_{ijk}^* can be defined using the damaged mode shapes. In order to account for all measured modes, the following formulation for the damage index for sub-region jk is used:

$$\beta_{jk} = \sum_{i=1}^{m} f_{ijk}^* \Big/ \sum_{i=1}^{m} f_{ijk}. \tag{23}$$

Once again a normalized damage index can be found using equation (14).

3. SIMULATION RESULTS

Both algorithms discussed in the theory section can be applied to detect damage in plate-like structures. The algorithm derived assuming plate-like behavior (2-D curvature) can be applied directly. To use the algorithm formulated assuming one-dimensional curvature the structure must be divided into "slices" and the algorithm needs to be applied to each slice individually. The normalized damage index is then determined using the average and standard deviation of all the damage indices from all the slices. The "slicing" algorithm is presented here for comparison only, because that would be the only way to apply the 1-D strain energy method to a plate-like structure. It is not expected that the slicing algorithm will perform well as it does not preserve the torsional stiffness between slices. Regardless of the method chosen several additional parameters must be chosen including the numbers of modes and the number of subdivisions to be used.

Several sets of simulated data were used to investigate the effectiveness of both approaches in locating damage in plate-like structures as well as to study the effect of changing the number of modes and subdivisions. The data were generated using a finite element model of a pinned–pinned plate with several elements reduced in stiffness to model damage. The finite element mesh is shown in Figure 3. The plate was given pinned boundary conditions at $y = -300$ and $y = 300$. The elements in the location of reduced stiffness are indicated in Figure 3. The reduced stiffness was in the region $48 < x < 96$, and $84 < y < 132$ with the center of the damage being located at $x = 72$, $y = 108$. All the analysis was done using MATLAB.

The first case studied had the stiffness of four elements reduced by 25%. The results from this case are shown in Figures 4–7. In all of these figures the normalized damage index is shown as a 3-D bar graph with values greater than 2 drawn in a darker color and are the likely locations of damage.

In Figure 4 the damage index is shown by dividing the structure into slices in the longitudinal direction of the plate, that is, slices with constant x values, with 20 divisions per slice and using just one mode. It is clear from Figure 4 that the algorithm does a fairly good job of locating the damage. The largest peak in Figure 4 has its center at a location of (72, 105). Increasing the number of modes

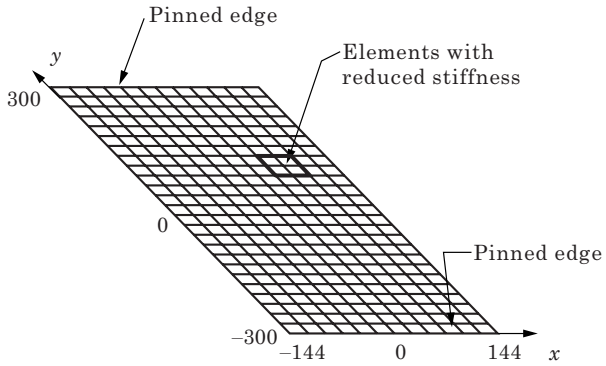

Figure 3. Finite element mesh of a pinned–pinned plate with an area of reduced stiffness.

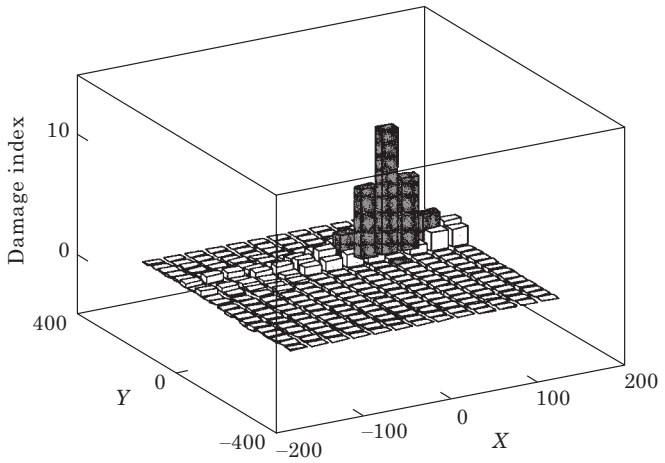

Figure 4. Damage index for a plate with a region of 25% reduced stiffness. The plate was divided into longitudinal slices, 20 divisions per slice, and one mode was used in the algorithm.

to five did not noticeably change the results. In Figure 5 the number of divisions per slice was increased to 40 and four modes are used. The results did not improve by increasing the divisions and the location of the damage was found to be roughly the same. When the structure was divided into slices in the transverse direction (i.e., constant y), 20 divisions/slice and using four modes, the damage was once again located as shown in Figure 6.

In Figure 7 the damage indices calculated using the algorithm derived for plate-like structures, one mode, and 20 divisions in each direction, are shown. Once again the damage is located fairly accurately. The two peaks in Figure 7 are located at (64·8, 105) and (79·2, 105). Clearly the choice of the number of divisions will affect the location of the peak. Once again, increasing the number of divisions and modes does not significantly improve the results.

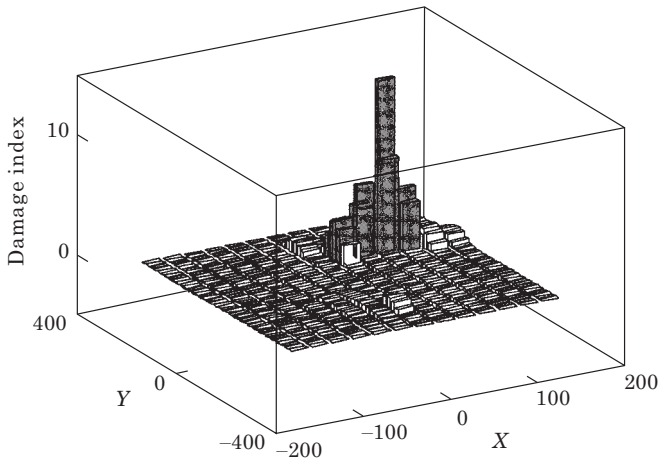

Figure 5. Damage index for a plate with a region of 25% reduced stiffness. The plate was divided into longitudinal slices, 20 divisions per slice, and four modes were used in the algorithm.

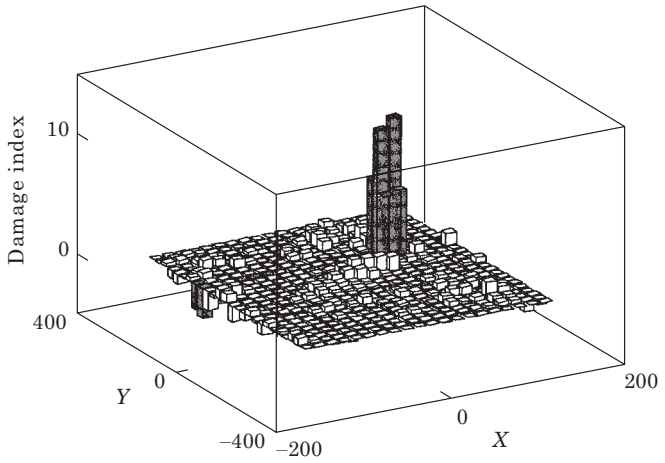

Figure 6. Damage index for a plate with a region of 25% reduced stiffness. The plate was divided into transverse slices, 20 divisions per slice, and four modes were used in the algorithm.

An example in which the method of dividing the structure into slices has several problems is examined in the second set of simulated data. In this case the stiffness was reduced by only 10%. The results of dividing the structure into longitudinal slices with 20 divisions/slice and using one and four modes are shown in Figures 8 and 9 respectively. In this case the region of reduced stiffness was not located when using just one mode and when additional modes were included the damage indices were found to be large along the node line of the second natural mode. In Figures 10, 11 the results using the algorithm for plate-like structures is shown. In Figure 10 only one mode was used and 20 divisions were used in both the x and y directions. From Figure 10 it is clear that the area

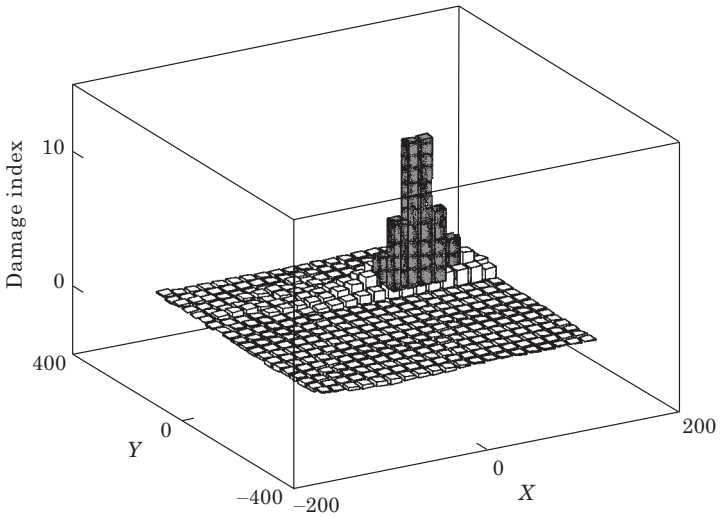

Figure 7. Damage index for a plate with a region of 25% reduced stiffness. The plate was divided into 20 divisions in each direction and the 2-D algorithm was used with one mode.

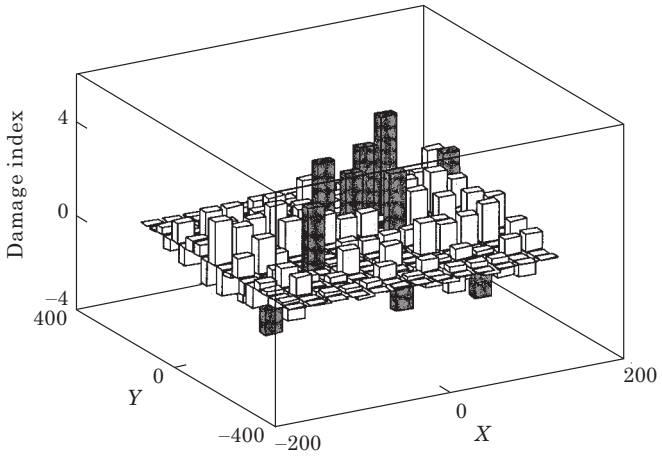

Figure 8. Damage index for a plate with a region of 10% reduced stiffness. The plate was divided into longitudinal slices, 20 divisions per slice, and one mode was used in the algorithm.

of reduced stiffness was not located. In Figure 11 four modes and 20 divisions in each direction were used in the 2-D algorithm and clearly the general location of the damage has been identified.

In all of the examples used thus far it was assumed that the mode shapes were known exactly on a very fine grid of sensors. In actual practice this will obviously not be the case. A reduced set of data was used to determine how the results change using a coarser grid of sensors. In this case the stiffness was reduced 25% and the number of sensor locations was reduced from 338 to 56. The results from dividing the structure into longitudinal slices with 20 divisions/slice and using four modes are shown in Figure 12. Once again, when more than one mode is used, the algorithm incorrectly identified damage as being along a

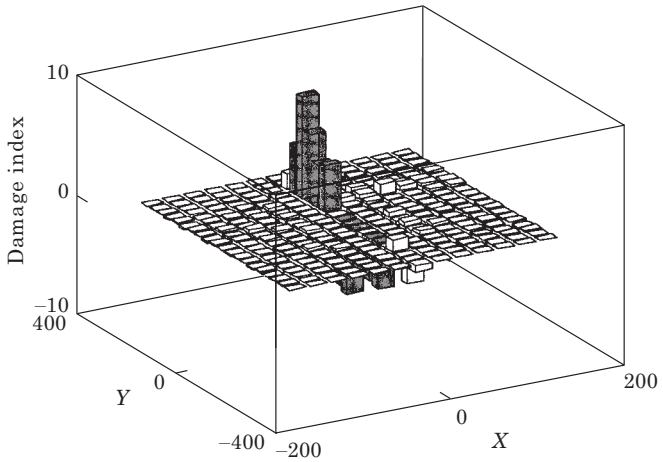

Figure 9. Damage index for a plate with a region of 10% reduced stiffness. The plate was divided into longitudinal slices, 20 divisions per slice, and four modes were used in the algorithm.

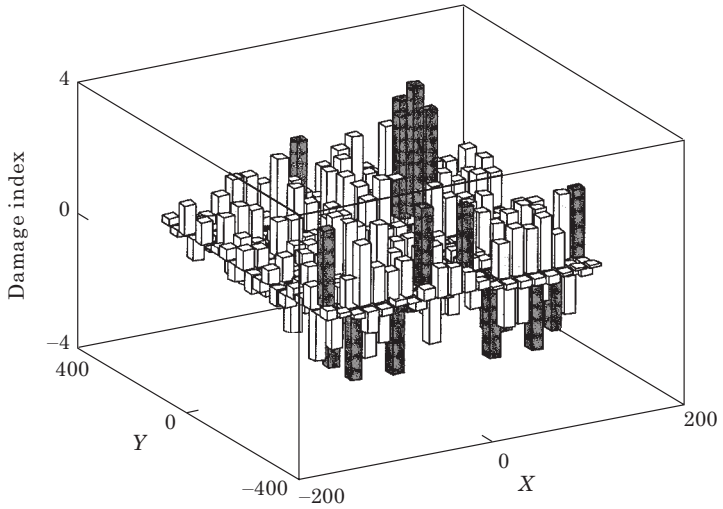

Figure 10. Damage index for a plate with a region of 10% reduced stiffness. The plate was divided into 20 divisions in each direction and the 2-D algorithm was used with one mode.

node line. Also, the resolution of this method is clearly limited by the number of slices that are available. Results from using the algorithm for 2-D curvature with four modes and 20 divisions in each direction are shown in Figure 13 and the general area of the damage can be clearly seen.

One of the major difficulties associated with implementing the algorithms discussed in this paper was the calculation of the derivatives and integrals when the mode shape is known at a relatively small number of discrete locations. In both algorithms additional intermediate points were calculated by curve-fitting

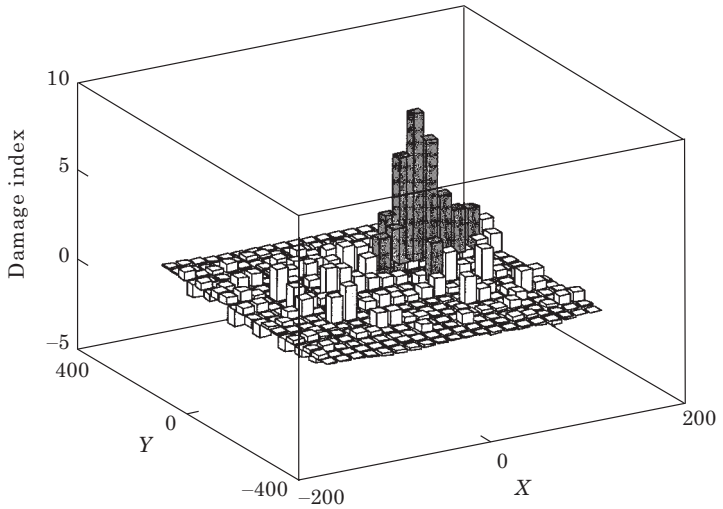

Figure 11. Damage index for a plate with a region of 10% reduced stiffness. The plate was divided into 20 divisions in each direction and the 2-D algorithm was used with four modes.

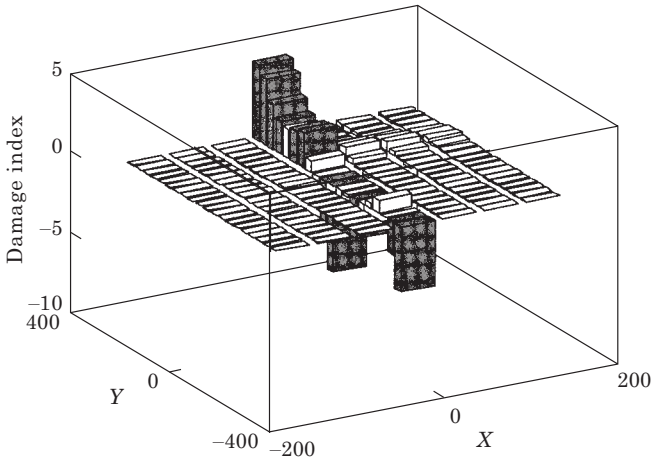

Figure 12. Damage index for a plate with a region of 25% reduced stiffness using a reduced number of sensors. The plate was divided into longitudinal slices, 20 divisions per slice, and four modes were used in the algorithm.

the data. The derivatives and integrals required by the algorithms were then calculated numerically.

4. EXPERIMENTAL SETUP AND RESULTS

To demonstrate the new technique experimentally, a $17\frac{3}{8}$ in. $\times$ $18\frac{1}{4}$ in. $\times$ $\frac{3}{8}$ in. aluminium plate was tested before and after a cut was made at two locations in the plate. The cut was made with a jeweler's saw and each end of the plate was clamped to an air bearing as shown in Figure 14. The use of air bearings was an attempt to have consistent boundary conditions throughout all the tests. Thirty-

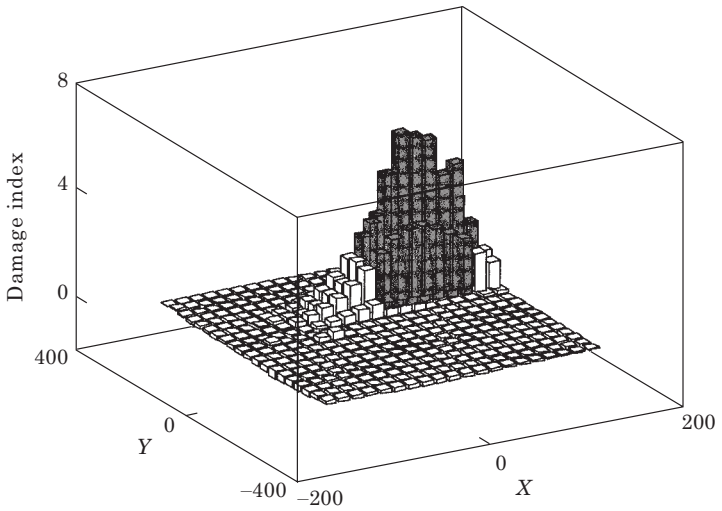

Figure 13. Damage index for a plate with a region of 10% reduced stiffness. The plate was divided into 20 divisions in each direction and the 2-D algorithm was used with four modes.

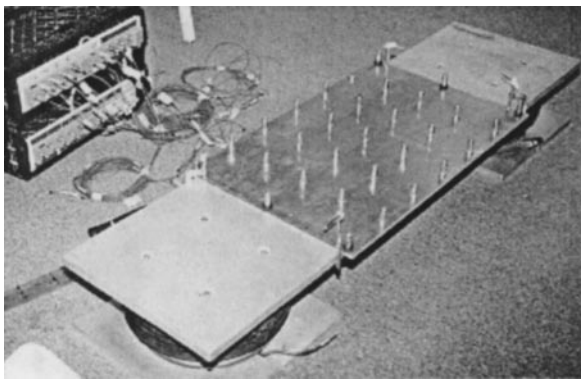

Figure 14. Experimental configuration of plate for damage identification tests.

one accelerometers were glued to the plate in the configuration shown in Figure 15. The impact location is also shown in Figure 15. Sawing diagonally at damage location one as shown in Figure 15 provided the initial damage for the structure. After this first cut additional damage was added to the plate at a second location, damage location two, as shown in Figure 15. A brief description of the eight damage cases studied is given in Table 1.

The test equipment used in this study consisted of a Hewlett-Packard (HP) 3566A dynamic data acquisition system including a model 35650 mainframe, 35653A source module, four 35653A 8-channel input modules which provided power for accelerometers and performed the analog to digital conversion of accelerometer signals, and a 35651C signal processing module that performed the needed Fast Fourier Transform calculations. A Toshiba Tecra 700CT Laptop was used for data storage and as a platform for the HP software that is the user interface for the data acquisition system.

The dynamic range for data acquisition was set by experimenting with different excitation levels and then setting the range so that response overloads were avoided. Wilcoxen Research model 736T accelerometers were used for the vibration measurements. This accelerometer has a nominal sensitivity of 10 mV/$\boldsymbol{g}$, an operating frequency of about 5–15 000 Hz, and an amplitude rate of 50 $\boldsymbol{g}$'s.

TABLE 1

Description of the damage cases studied for the plate

Number	Description
1	1 in. long cut at location 1
2	2 in. long cut at location 1
3	Cut extends to 1/4 in. from the edge of the plate at location 1
4	Cut is all the way through the edge at location 1
5	0·75 in. cut at location 2
6	1·75 in. cut at location 2
7	Cut extends to 1/4 in. from the edge of the plate at location 2
8	Cut is all the way through the edge at location 2

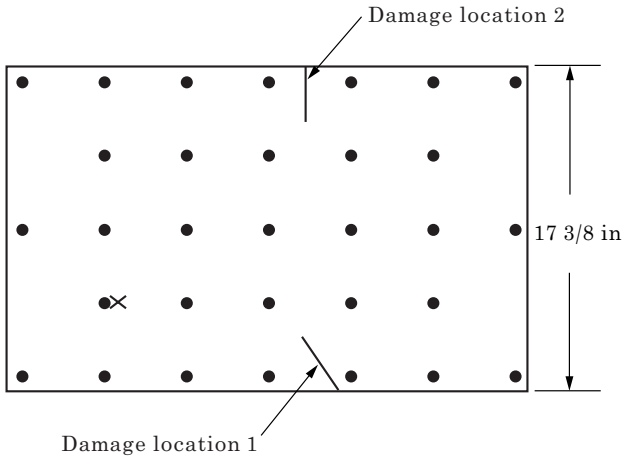

Figure 15. Experimental schematic of plate for damage identification tests. X, Impact location; ●, accelerometer locations.

Lengths of MicroDot cable were used to connect the accelerometers to the input modules.

The system samples the analog signal from the accelerometers at approximately 32 kHz (regardless of the frequency range being analyzed), passes the signal through an analog anti-aliassing filter, digitizes it, then passes the data through a digital anti-aliassing filter with the cutoff frequency based upon the Nyquist frequency for the specified sampling parameters. The signal is then decimated based on the particular sampling parameters.

The data acquisition system was set up to measure acceleration–time histories and a force–time history of the input, and to calculate the frequency–response functions (FRF's) of these time histories. Testing parameters were specified as 10 averages discretized with 1024 samples. A force window was applied to the signal from the impact hammer's force transducer and an exponential window was applied to the signal from the accelerometers. The 1024 time samples yielded 512 spectral points, but because of the rolloff in the anti-aliassing filters, only 401 spectral points are displayed.

The curve fitting and modal extraction were done using the software program, DIAMOND [12]. Although a variety of methods are available in this code (ERA, rational polynomial, and complex exponential), the rational polynomial method was the only one used.

The structure was tested several times in an undamaged state and then again after each saw cut. The strain energy method was applied to the data and the results are shown in Figures 16–19.

This method clearly identified both damage locations for damaged case 8, but only identified the 1st damage location for damage case 7. Evidently the change in mode shape curvature due to the damage at the first location dominated the results until the damage at the second location was roughly comparable in severity. This indicates that this method has problems identifying multiple damage locations of different degrees of severity. The smallest case of damage

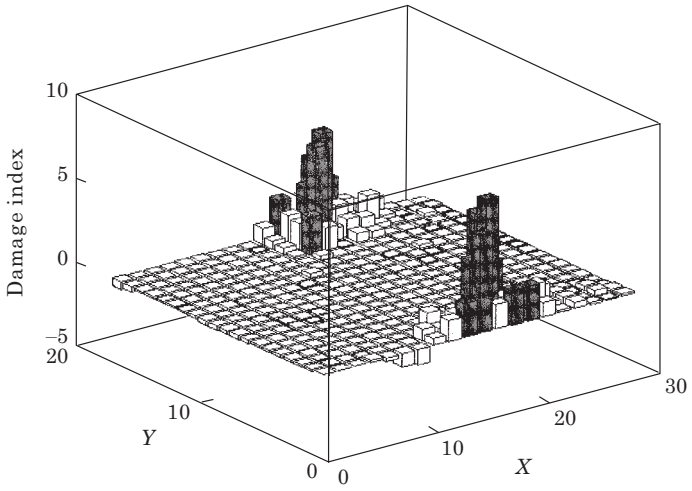

Figure 16. Experimentally determined damage index for damage case 8. The plate was divided into 20 divisions in each direction and the 2-D algorithm was used with 12 modes.

that was identified was damage case 3. Clearly in damage case 2 the damage is not identified and some false positives appear at locations other than the damage location. Without prior knowledge there is no way to determine which is the true damage and which is a false positive.

Overall, the 2-D strain energy method performed comparably to the historical performance of the 1-D strain energy method [5]. Specifically, the method showed a propensity for false-positive results (especially at low levels of damage), but generally performed well as the level of damage increased.

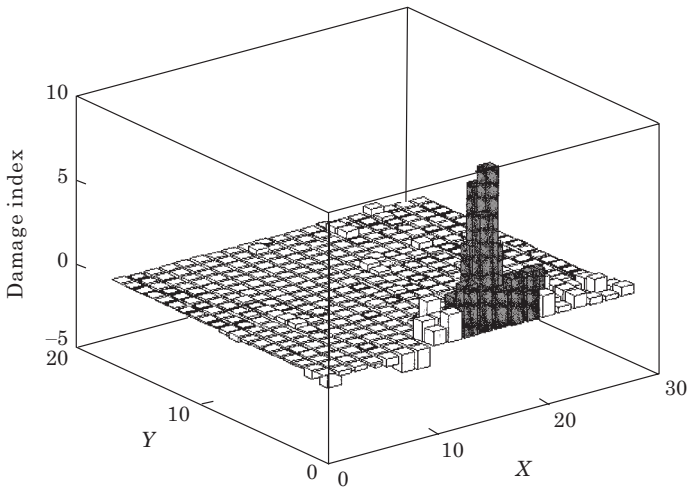

Figure 17. Experimentally determined damage index for damage case 7. The plate was divided into 20 divisions in each direction and the 2-D algorithm was used with 11 modes.

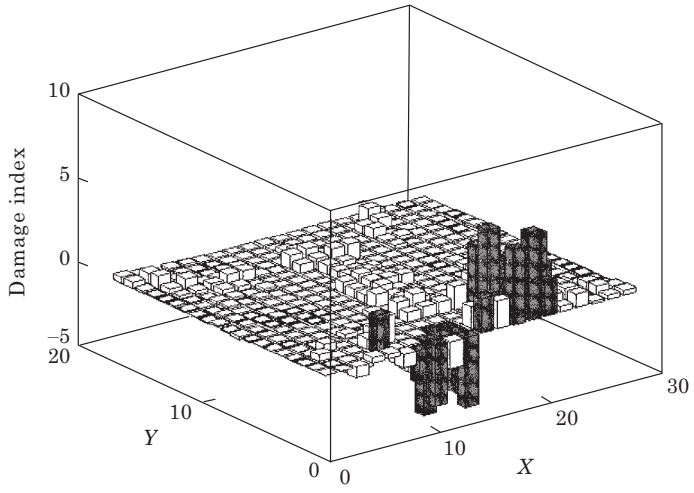

Figure 18. Experimentally determined damage index for damage case 3. The plate was divided into 20 divisions in each direction and the 2-D algorithm was used with 12 modes.

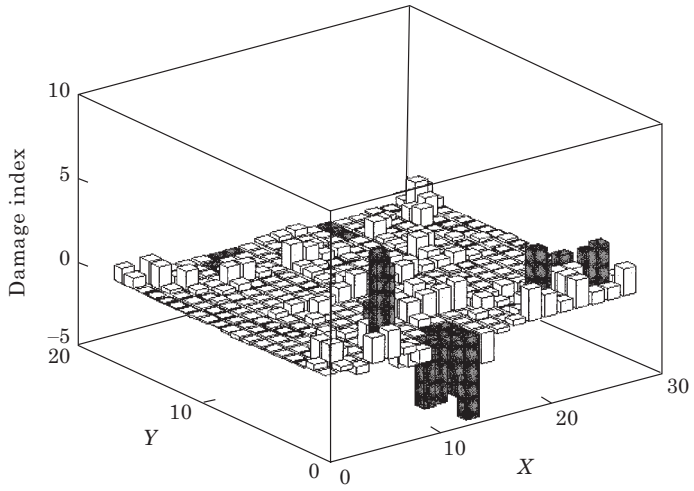

Figure 19. Experimentally determined damage index for damage case 2. The plate was divided into 20 divisions in each direction and the 2-D algorithm was used with 12 modes.

5. CONCLUSIONS

A damage detection algorithm derived for structures whose modes are characterized by one-dimensional curvature has been generalized for plate-like structures that are characterized by two-dimensional curvature. The method only requires the mode shapes of the structure before and after damage and the modes do not need to be mass normalized making it very advantageous when using ambient excitation. The algorithm was found to be effective in locating areas with stiffness reductions as low as 10% using relatively few modes. The algorithm was also demonstrated successfully using experimental data.

ACKNOWLEDGMENTS

Funding for this research was provided by the Department of Energy through the Los Alamos National Laboratory's Laboratory Directed Research and Development (LDRD) program.

REFERENCES

1. S. W. Doebling, C. R. Farrar and M. B. Prime 1998 *The Shock and Vibration Digest* **30**(2), 91–105. A summary review of vibration-based damage identification methods.
2. A. K. Pandey, M. Biswas and M. M. Samman 1994 *Journal of Sound and Vibration* **154**, 321–332. Damage detection from changes in curvature mode shapes.
3. N. Stubbs, J.-T. Kim and K. Topole 1992 *Proceedings of the ASCE Tenth Structures Congress*, 543–546. An efficient and robust algorithm for damage localization in offshore platforms.
4. N. Stubbs, J.-T. Kim and C. R. Farrar 1995 *Proceedings of the* 13*th International Modal Analysis Conference*, 210–218. Field verification of a nondestructive damage localization and sensitivity estimator algorithm.
5. D. V. Jauregui and C. R. Farrar 1996 *Proceedings of the* 14*th International Modal Analysis Conference*, 119–125. Damage detection algorithms applied to numerical modal data from a bridge.
6. D. V. Jauregui and C. R. Farrar 1996 *Proceedings of the* 14*th International Modal Analysis Conference*, 1423–1429. Comparison of damage identification algorithms on experimental modal data from a bridge.
7. J. Chance, G. R. Tomlinson and K. Worden 1994 *Proceedings of the* 12*th International Modal Analysis Conference*, 778–785. A simplified approach to the numerical and experimental modeling of the dynamics of a cracked beam.
8. I. Kondo and T. Hamamoto 1994 *Proceedings of the fourth International Offshore and Polar Engineering Conference* **4**, 400–407. Local damage detection of flexible offshore platforms using ambient vibration measurements.
9. O. S. Salawu and C. Williams 1994 *Proceedings of the* 12*th International Modal Analysis Conference*, 933–939. Damage location using vibration mode shapes.
10. D. I. Nwosu, A. S. J., Swamidas, J. Y. Guigne and D. O. Olowokere 1995 *Proceedings of the* 13*th International Modal Analysis Conference*, 1122–1128. Studies on influence of cracks on the dynamic response of tubular T-joints for nondestructive evaluation.
11. D. Young 1956 *Journal of Applied Mechanics*, 448–453. Vibration of rectangular plates by the Ritz method.
12. S. W. Doebling, C. R. Farrar and P. J. Cornwell 1997 *Proceedings of the Sixth International Conference on Recent Advances in Structural Dynamics*, 399–412. DIAMOND: A graphical user interface toolbox for comparative modal analysis and damage identification.